Electronic Supplementary Information

Single band ratiometric luminescence thermometry based on Pr^{3+} doped oxides containing charge transfer states

Jiawen Wang,[ab] Junyi Li,[b] Ruoshan Lei,*[b] Shilong Zhao [b] and Shiqing Xu *[b]

[a] *College of Materials and Chemistry, China Jiliang University, Hangzhou, 310018, China*

[b] *Institute of Optoelectronic Materials and Devices, China Jiliang University, Hangzhou, 310018, China*

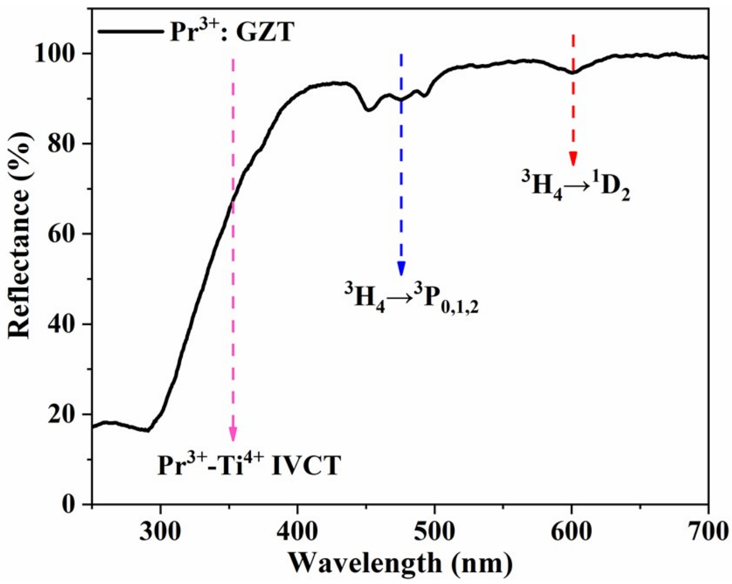

Fig. S1. Diffuse reflectance spectrum of the Pr^{3+}: GZT phosphor.

Supplementary Note 1. The calculation of IVCT energy. According to previous studies, the position of the IVCT band will affect the electron distribution between the $^3P_0$ and $^1D_2$ energy levels. Boutinaud et al. have proposed an empirical equation to evaluate the energy of Pr^{3+}-Ti^{4+} IVCT as follows:[1,2]

$$IVCT(cm^{-1}) = 58800 - 49800\left[\frac{\chi(Ti^{4+})}{d(\mathrm{Pr}^{3+} - Ti^{4+})}\right] \qquad \text{(S1)}$$

where $\chi(Ti^{4+})$ is the optical electronegativity of Ti^{4+} (2.05), and $d(\mathrm{Pr}^{3+} - Ti^{4+})$ is the average distance between Pr^{3+} and Ti^{4+}. For Pr^{3+}: GZT, the mean distance between Gd^{3+}-Ti^{4+} is ~3.37 Å based on the crystal structure data (ICSD-251934).[3] Accordingly, the calculated IVCT energy is ~351 nm (28520 cm^{-1}), which is consistent with the experimental data detected in the excitation spectrum (340 nm, 29412 cm^{-1}).

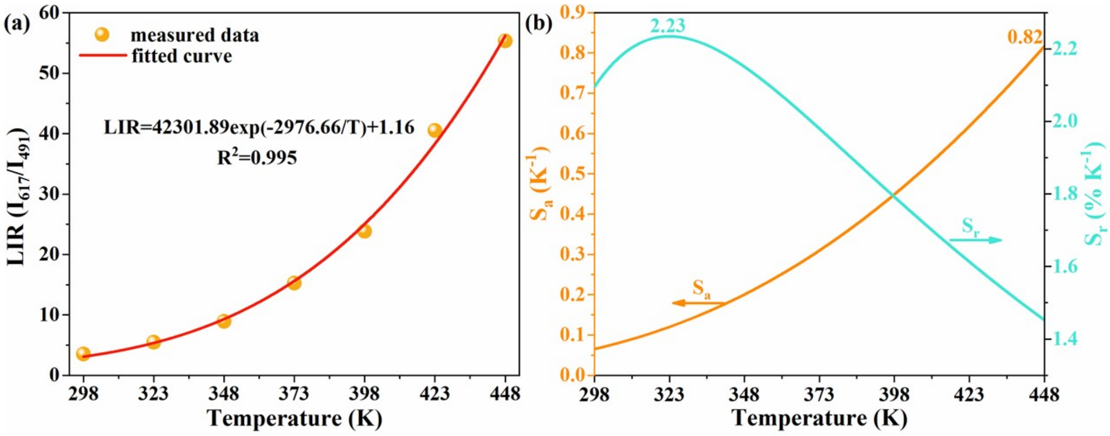

Fig. S2. (a) Experimentally measured and fitted plot of $LIR=I_{617}/I_{491}$ versus temperature. (b) The corresponding S_a and S_r as a function of temperature.

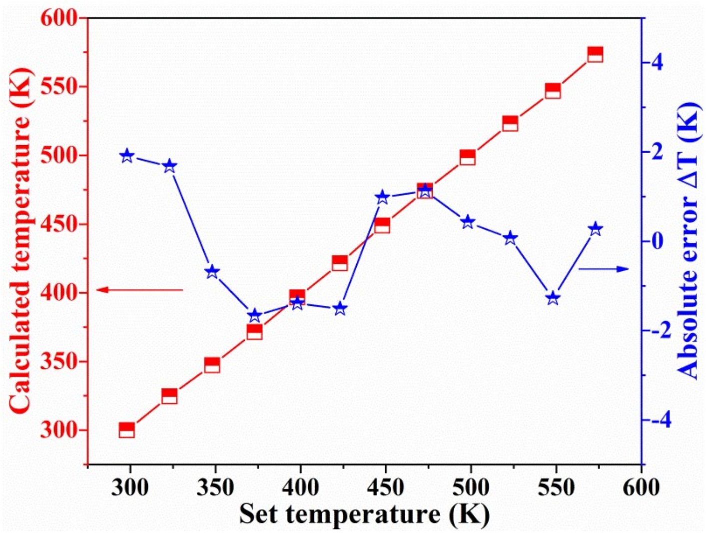

Fig. S3. Absolute error (ΔT) as a function of temperature for $LIR_{^3P_0\rightarrow{}^3H_4}(\mathrm{I}_{EX:f-f}/\mathrm{I}_{EX:IVCT})$ data.

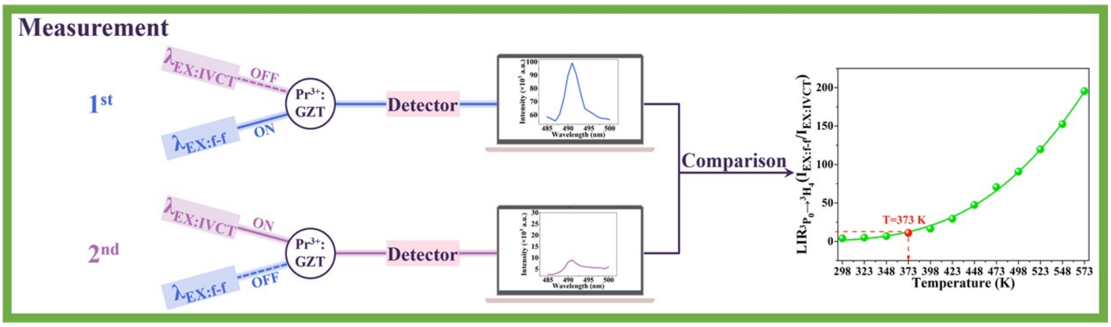

Fig. S4. Schematic diagram of the present SBR method in Pr^{3+}: GZT.

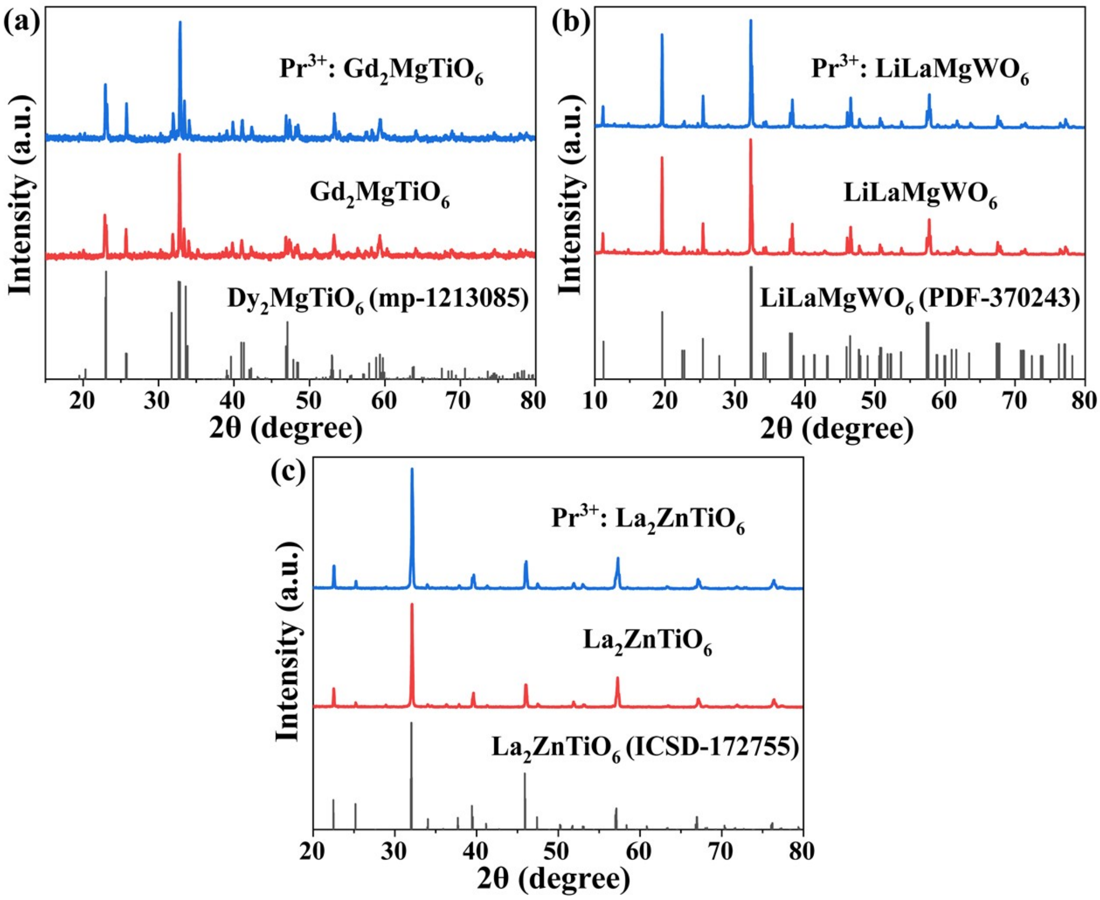

Fig. S5. (a) XRD patterns of Gd_2MgTiO_6 and Pr^{3+}: Gd_2MgTiO_6 samples. Due to the lack of structural information of Gd_2MgTiO_6 in the crystal database, the standard data of Dy_2MgTiO_6 with an analogous structure (mp-1213085) is used as a reference. (b) XRD patterns of $LiLaMgWO_6$ and Pr^{3+}: $LiLaMgWO_6$ samples, and the standard data of $LiLaMgWO_6$ (PDF-370243) is used as a reference. (c) XRD patterns of La_2ZnTiO_6 and Pr^{3+}: La_2ZnTiO_6 samples with the standard data of La_2ZnTiO_6 (ICSD-172755) as a reference.

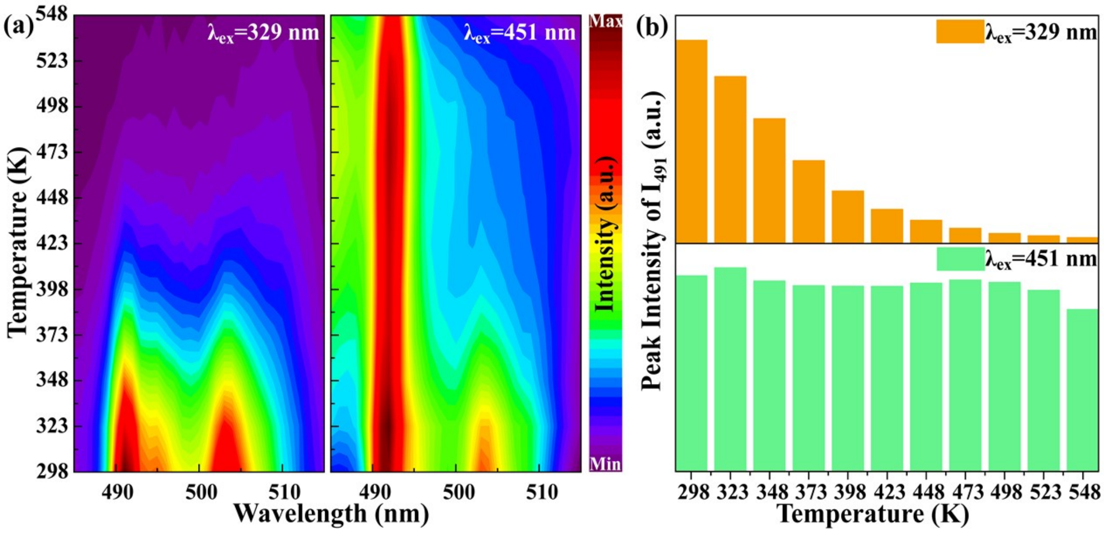

Fig. S6. (a) Temperature-dependent PL spectra of Pr^{3+}: Gd_2MgTiO_6 upon the excitations of Pr^{3+}-Ti^{4+} IVCT (λ_{ex}=329 nm) and Pr^{3+}: $^3H_4 \rightarrow ^3P_2$ transition (λ_{ex}=451 nm). (b) Temperature-variational intensities of the 491 nm emission (Pr^{3+}: $^3P_0 \rightarrow ^3H_4$ transition) under two different excitation lines (λ_{ex}=329 and 451 nm).

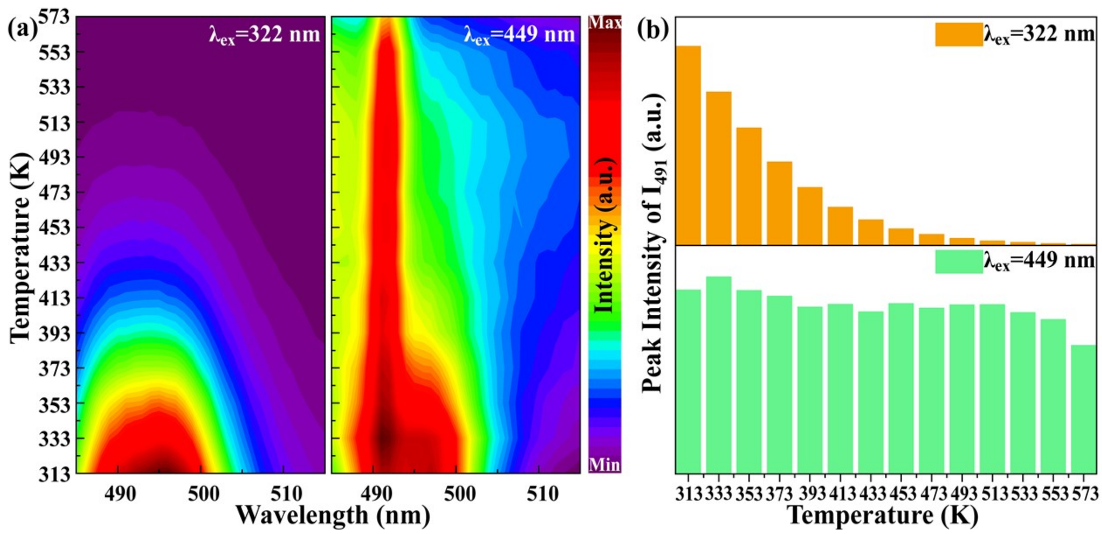

Fig. S7. (a) Temperature-dependent PL spectra of Pr^{3+}: $LiLaMgWO_6$ upon the excitations of Pr^{3+}-W^{6+} IVCT (λ_{ex}=322 nm) and Pr^{3+}: $^3H_4 \rightarrow ^3P_2$ transition (λ_{ex}=449 nm). (b) Temperature-variational intensities of the 491 nm emission (Pr^{3+}: $^3P_0 \rightarrow ^3H_4$ transition) under two different excitation lines (λ_{ex}=322 and 449 nm).

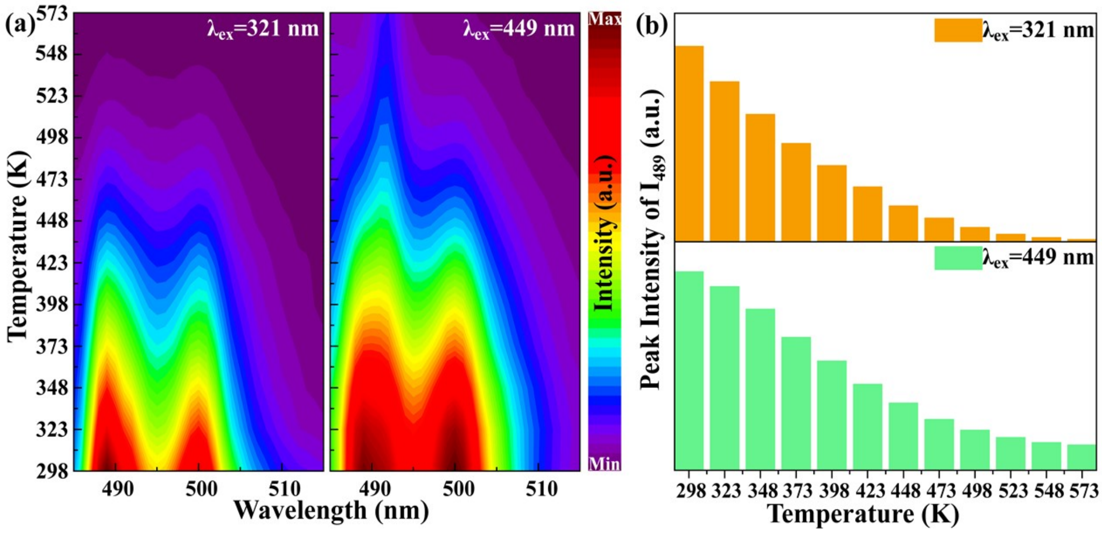

Fig. S8. (a) Temperature-dependent PL spectra of Pr^{3+}: La_2ZnTiO_6 upon the excitations of the Pr^{3+}-Ti^{4+} IVCT state (λ_{ex}=321 nm) and Pr^{3+}: $^3H_4 \rightarrow {}^3P_2$ transition (λ_{ex}=449 nm). (b) Temperature-variational intensities of the 489 nm emission (Pr^{3+}:$^3P_0 \rightarrow {}^3H_4$ transition) under two different excitation lines (λ_{ex}=321 and 449 nm).

References

1 Y. Gao, F. Huang, H. Lin, J. Xu and Y. Wang, Sens. Actuators B Chem., 2017, **243**, 137-143.

2 R. Shi, L. Lin, P. Dorenbos and H. Liang, J. Mater. Chem. C, 2017, **5**, 10737-10745.

3 N. Das, M. A. Nath, G. S. Thakur, M. Thirumal and A. K. Ganguli, J. Solid State Chem., 2015, **229**, 97-102.